

# Development of a self-balancing robot with a control moment gyroscope

Ji-Hyun Park<sup>1</sup> and Baek-Kyu Cho<sup>2</sup>

## Abstract

This study introduces a two-wheeled self-balancing mobile robot based on a control moment gyroscope module. Two-wheeled mobile robots are able to achieve better mobility and rotation in small spaces and to move faster than legged robots such as humanoid type robots. For this reason, the two-wheeled mobile robot is generally used as a mobile robot platform. However, to maintain its balance, the two-wheeled robot needs to use movements of its two wheels. When an unexpected disturbance affects the robot, the robot maintains its balance with movements of the wheels and tilting of the body. If the disturbance exceeds the response capability of the robot, the robot will lose its stability. At the same time, the safety of the robot may be put at risk by movements to maintain balance. To address these issues, a robot was designed with a control moment gyroscope module to improve balance while minimizing movement. When a disturbance is applied to the robot, the disturbance is estimated by a disturbance observer and the control moment gyroscope controller compensates the disturbance. Using the control moment gyroscope module, the robot can maintain balance with just small movements of its wheels. Improved performance and stability were verified with experiments and simulations.

## Keywords

Self-balancing robot, control moment gyroscope, disturbance observer, KUWAY

Date received: 7 September 2017; accepted: 4 March 2018

Topic: Special Issue – Mobile Robots

Topic Editor: Lino Marques

Associate Editor: Michal Kelemen

## Introduction

Wheeled mobile robots have a significant advantage over humanoid type robots, in that they are faster and can more easily change direction while moving, and this makes them very useful for a number of applications. Among wheeled robots, two self-balancing robots, the Segway and Ninebot, have become popular and are used for commuting or as patrol transporters.<sup>1,2</sup> In addition, self-balancing wheeled robots such as Anybots QB are currently used as a service robot platform.<sup>3,4</sup> Due to their increasing popularity, advanced self-balancing robots are currently being developed as well. The Golem Krang was developed at the Georgia Institute of Technology. Its base is similar to a normal two-wheeled self-balancing robot, but it has anthropomorphic arms.<sup>5</sup> The two wheels of the robot are used to balance the body and the robotic arm, which is fixed to the

upper body, is designed to perform tasks such as removing obstacles. The Ballbot was developed at Carnegie Mellon University. This robot system is designed to balance on a sphere, which makes it particularly easy to switch orientation and move in any direction.<sup>6</sup> In addition, KAIST has developed a two-wheeled self-balancing robot that has an

<sup>1</sup>Field Robotics R&D Division, Korea Institute of Robot and Convergence, Pohang, South Korea

<sup>2</sup>School of Mechanical Engineering, Kookmin University, Seoul, South Korea

### Corresponding author:

Baek-Kyu Cho, Robotics and Control Laboratory, School of Mechanical Engineering, Kookmin University, 77, Jeongneung-ro, Seongbuk-gu, Seoul, South Korea.

Email: swan0421@gmail.com



Creative Commons CC BY: This article is distributed under the terms of the Creative Commons Attribution 4.0 License

(<http://www.creativecommons.org/licenses/by/4.0/>) which permits any use, reproduction and distribution of the work without further permission provided the original work is attributed as specified on the SAGE and Open Access pages (<https://us.sagepub.com/en-us/nam/open-access-at-sage>).

upper body with five degrees-of-freedom. By using its upper body, the robot maintains a dynamic balance based on the zero-moment point.<sup>7</sup>

As different types of self-balancing robots become more frequently used in various fields and different environments, it is increasingly important to prevent accidents. It is well-known that the owner of Segway Inc., Jimi Heselden, died in an accidental fall while riding a Segway in 2010. In similar accidents, when the self-balancing robot encounters an unexpected disturbance, it can lose its stability. Even though more robust control algorithms for the self-balancing robot have been developed for stability,<sup>8,9</sup> they do not perfectly guarantee safety. For example, the robust algorithm can guarantee better stability against disturbances. But, because of the characteristics of the self-balancing robot, the robot has to move its wheels and tilt its body to keep balance. It cannot stay in one place while responding to an external force.<sup>10</sup> It is obvious that the larger the disturbance, the more the robot moves. Even when the robot is located in front of a cliff or a human, if a disturbance is applied to the robot, the robot has to move itself to keep balance, and in that case, there is a risk that the robot will fall or hit the human. In other words, even when the robot maintains its stability, it can become unsafe.<sup>11,12</sup> And For this reason, it is important that the control algorithm not only keeps the self-balancing robot stable but also ensures that it maintains its position. Thus, it has to be equipped with additional hardware to guarantee both stability and safety at the same time.

Representative self-balancing robots which have additional equipment for balancing include the Murata Boy developed by Murata of Japan<sup>13</sup> and the C1 developed by Lit Motors, USA.<sup>14,15</sup> The Murata Boy is a robot that has a flywheel mounted on the body riding a bicycle. The flywheel generates torque around the roll axis and this enables the robot to control its posture along the roll axis. The C1 is a motorcycle having an electrically controlled control moment gyroscope (CMG). The CMG generates torque via a rotating flywheel and gimbal and is mainly used for attitude control of satellites and for roll control of large ships, because it can generate higher torque more precisely than a flywheel. Using the CMG prevents the C1 from falling down in accident situations. In addition, the CMG makes it easier to drive at low speed and maintain balance while stopping because it controls balance along the roll axis. However, because of the CMGs characteristics, the CMG cannot be used for continuous or constant disturbances.<sup>16</sup>

This article introduces the development of a two-wheeled self-balancing robot, called the Kookmin University segWAY (KUWAY), which employs CMG to generate torque around the pitch (left–right) axis. The KUWAY is shown in Figure 1. Even though most systems having CMG use it to generate torque around the roll axis, in the KUWAY, the CMG generates torque around the pitch axis. As a result, the KUWAY can maintain its balance against a

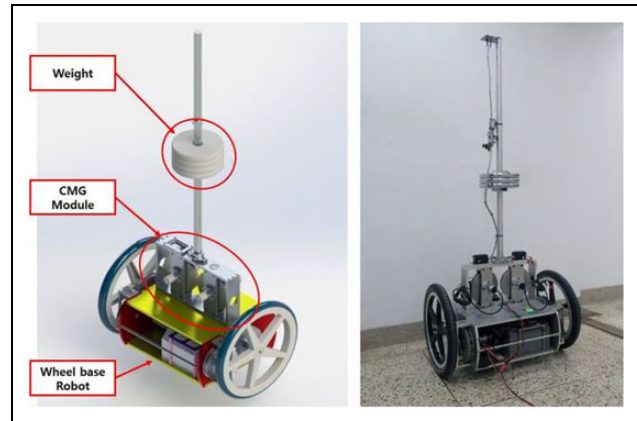


**Figure 1.** KUWAY. KUWAY: Kookmin University segWAY.

disturbance while using minimized movement. That is, it guarantees both stability and safety.

## Hardware

The KUWAY introduced in this article is a two-wheeled self-balancing robot with CMG. It is comprised of two main parts, a self-balancing robot and a CMG module, as shown in Figure 2. The main controller (TMS320F2808 developed by Texas Instrument) controls the self-balancing algorithm of the robot and the CMG module. A detailed explanation for each part is provided below. And the communication part act that the KUWAY communicates with laptop using Bluetooth to observe the status of KUWAY in Figure 2. This allows the state of the KUWAY to be monitored in real time while the robot is operating.

### Self-balancing robot

The self-balancing robot part is similar to other typical two-wheeled self-balancing robots, such as the Segway. Its role is to maintain balance using movement of the wheels and body. It is driven by two actuators consisting of a DC motor and a pulley/belt mechanism. The DC motors are Ampflow DC motors (A28-150) operated at 24 V and have 3 HP (2.2 kW) power. The motor has a maximum speed of 6100 rpm and a maximum torque of 13.9 Nm.

To increase the torque of the actuator, a pulley/belt mechanism was adopted. The reduction ratio was set to about 10:1. Because of the limited size of the pulley, two pulley/belt mechanisms were serially connected. Thus, the reduction ratio of the single pulley/belt mechanism was selected to be 3.14:1 (44:14) and the final reduction ratio became 9.88:1 (44<sup>2</sup>:14<sup>2</sup>). Both motors have a rotary encoder of 1000 ppr to measure angle.

In order to measure the tilt angle and angular velocity of the robot, an inertia measurement unit (IMU) was developed. The IMU consists of an inclinometer (DAS, M1) and a gyro sensor (Silicon Sensing Systems, CRS 03-02). Even though the inclinometer can accurately measure the tilt angle of the body, it cannot measure the correct angle

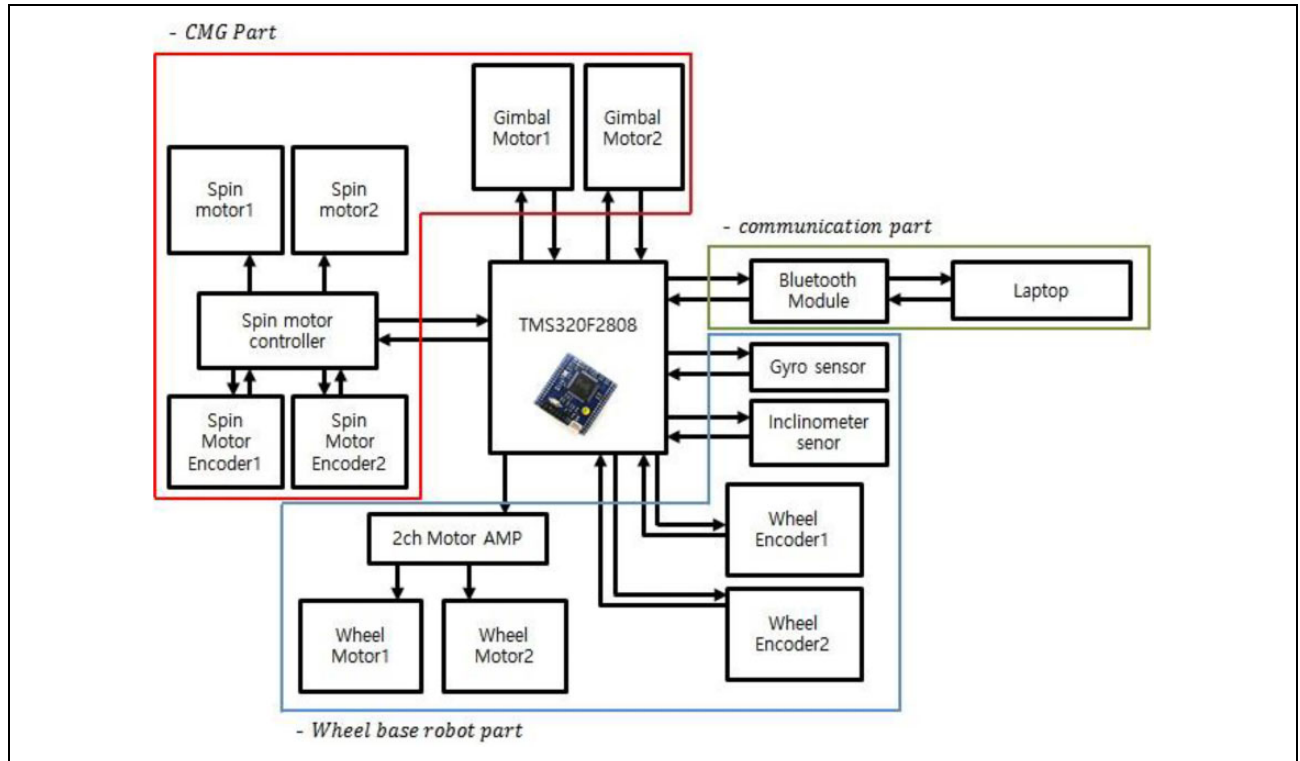


**Figure 2.** A block diagram of KUWAY. KUWAY: Kookmin University segWAY.

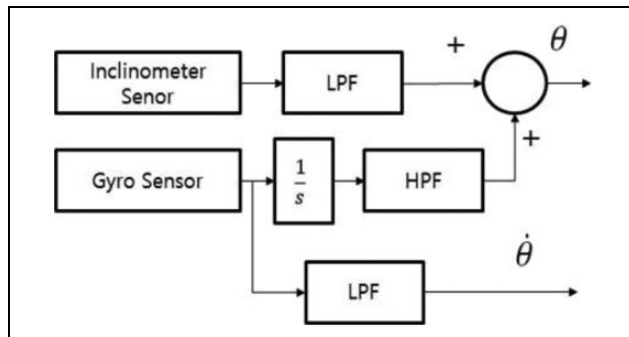


**Figure 3.** A block diagram of the complementary filter.

during fast rotation because of centrifugal force. On the other hand, the gyro sensor used to measure the angular velocity of the body can estimate the angle of the body by integrating angular velocity. However, drift may occur due to the accumulation of errors in the steady state.

In order to compensate the limitations of the two sensors, a complementary filter was applied as shown in Figure 3. The complementary filter has a low-pass filter for the inclinometer and a high-pass filter for the gyro sensor. The cut-off frequencies of both filters were determined experimentally. In this article, the cut-off frequency is decided to 0.2 Hz.

### CMG module

The CMG module used in the KUWAY is shown in Figure 4. It was placed on the self-balancing robot as

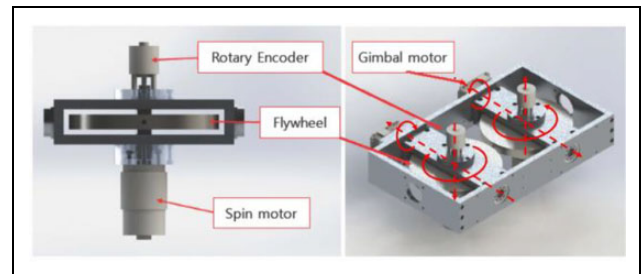


**Figure 4.** The CMG. CMG: control moment gyroscope.

shown in Figure 1. The module consists of two CMGs and each CMG has two actuators. One actuator rotates the flywheel and the other rotates the gimbal where the flywheel is contained. The CMG generates torque in a direction perpendicular to the rotational axes of the flywheel and gimbal. The magnitude of the torque is the product of the angular velocity of the gimbal and the momentum of the flywheel. In order to generate enough torque, it is necessary to have a bigger moment of inertia and/or a faster flywheel speed. To ensure that the torque of the CMG is accurate, the two flywheels need to rotate at a constant speed. For this reason, each flywheel was equipped with a 270W DC motor (RS-775wc, MABUCHI) and a rotary encoder to control rotation. The gimbal motor used in the CMG does not need high speed, just sufficient torque, so the DYNAMIXEL MX-106T from Robotis was selected.

## Modeling of KUWAY

### Modeling of self-balancing robot

When the two-wheeled self-balancing robot encounters a disturbance, its stability is mainly affected by disturbances which are applied in the back and forth directions. Therefore, the stability and the safety of the KUWAY were dominantly handled in the sagittal plane. Figure 5 shows a free body diagram of the self-balancing robot of the KUWAY in the sagittal plane. Equations (1) and (2) are the equations of motion applied with the motor dynamics

$$(Ml_{CG}^2 + I_{CG} + 2n^2J_m)\ddot{\theta} + (Mrl_{CG}\cos\theta - 2n^2J_m)\ddot{\phi} + 2n^2\left(k_f + \frac{k_t k_v}{R}\right)\dot{\theta} - 2n^2\left(k_f + \frac{k_t k_v}{R}\right)\dot{\phi} - Mgl_{CG}\sin\theta + F_d d \cos\theta = -2n\frac{k_t}{R}V \quad (1)$$

$$[2J + (2m + M)r^2 + 2n^2J_m]\ddot{\phi} + (Mrl_{CG}\cos\theta - 2n^2J_m)\ddot{\theta} - 2n^2\left(k_f + \frac{k_t k_v}{R}\right)\dot{\theta} + 2n^2\left(k_f + \frac{k_t k_v}{R}\right)\dot{\phi} - Mrl_{CG}\sin\theta\dot{\theta}^2 + F_d r = 2n\frac{k_t}{R}V \quad (2)$$

where  $\theta$  is the tilt angle of the body,  $\phi$  is the rotational angle of the wheel, and  $F_d$  is the disturbance. The parameters of the KUWAY are summarized in detail in Table. 1.

### Modeling of the CMG

In the KUWAY, the CMG generates torque on the basis of precessional motion. That is, when the flywheel rotates (along the  $z'$ -axis in Figure 6) and the gimbal containing the flywheel rotates along a direction perpendicular to the rotational axis of the flywheel ( $y$ -axis), the torque is generated along the direction of the cross product of both vectors ( $x'$ -axis). Figure 6 shows a free body diagram of a single CMG. If the angular velocity of the gimbal is denoted as  $\vec{\Omega}$  and the momentum of the flywheel is denoted as  $\vec{H}$ , the torque generated by the CMG,  $\vec{T}_{CMG}$ , is expressed as follows

$$\vec{T}_{CMG} = \vec{\Omega} \times \vec{H} = \dot{\theta}_{gb}\omega I_z \cos\theta_{gb}\vec{i} - \dot{\theta}_{gb}\omega I_z \sin\theta_{gb}\vec{k} \quad (3)$$

where

$$\vec{\Omega} = \dot{\theta}_{gb}\vec{j}$$

$$\vec{H} = \omega I_z \cos\theta_{gb}\vec{k} + \omega I_z \sin\theta_{gb}\vec{i}$$

Here,  $\theta_{gb}$  is the angle of the gimbal,  $\omega$  is the angular velocity of the flywheel, and  $I_z$  is the moment of inertia of the flywheel around the rotational axis.

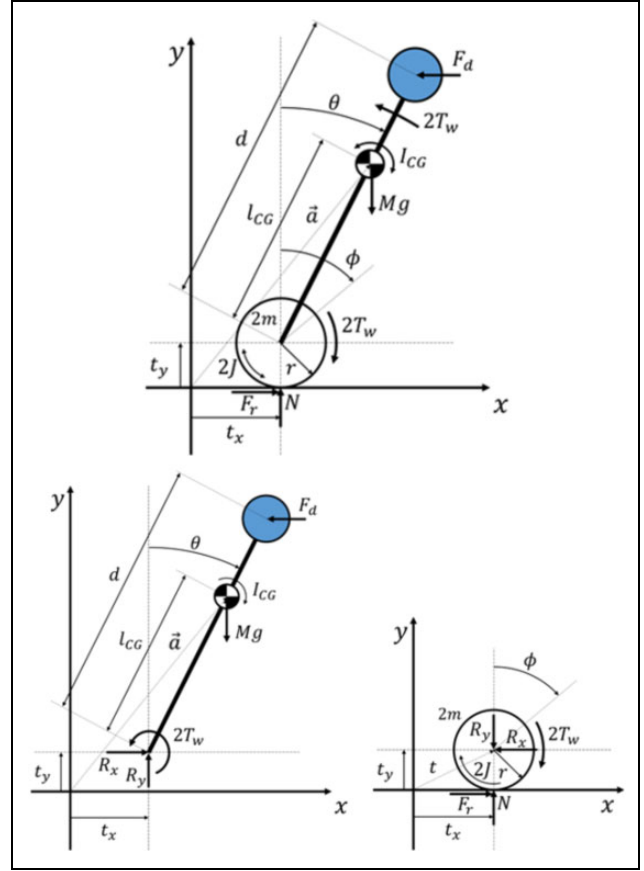


**Figure 5.** A free body diagram of the self-balancing robot of the KUWAY in the sagittal plane. KUWAY: Kookmin University segWAY.

**Table 1.** The parameters of the KUWAY.

Symbol	Parameter
$\theta$	Angle of the body
$\phi$	Angle of the wheel
$M$	Mass of the body
$l_{CG}$	Length of the wheel axis and center of mass
$I_{CG}$	Moment of inertia of the body
$J_m$	Moment of inertia of the rotor in a motor
$m$	Mass of the wheel
$J$	Moment of inertia of a wheel
$r$	Radius of a wheel
$n$	Reduction ratio
$k_f$	Damping constant of a motor
$k_t$	Torque constant of a motor
$k_v$	Back EMF constant of a motor
$R$	Resistor of a motor
$d$	Length of the wheel axis and a disturbance point
$V$	Voltage of a motor
$g$	Gravity

KUWAY: Kookmin University segWAY.

Because of the angle of the gimbal ( $\theta_{gb}$ ), the torque,  $\vec{T}_{CMG}$ , has the  $x$ - and  $z$ - directional components. Since the CMG in the KUWAY was designed to generate torque

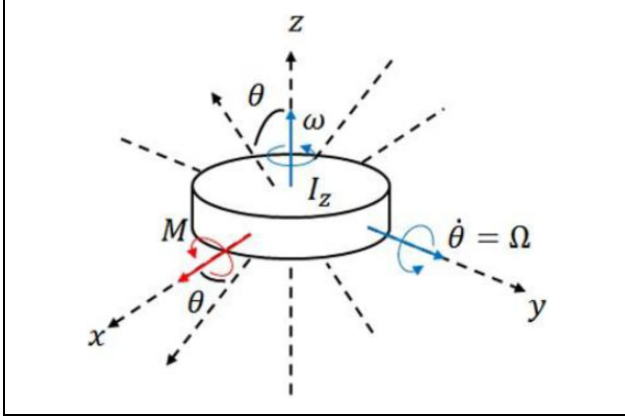


**Figure 6.** Free body diagram of single CMG. CMG: control moment gyroscope.

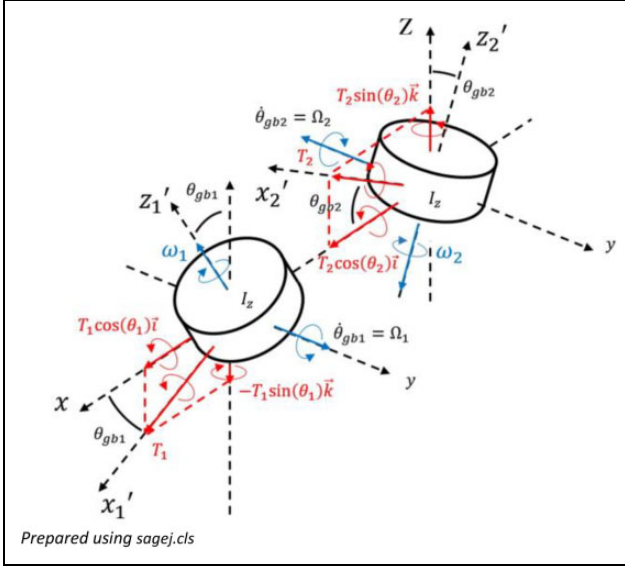


**Figure 7.** Free body diagram of two CMGs. CMG: control moment gyroscopes.

around the pitch axis, only one component of the torque is needed in equation (3). Therefore, the undesirable component has to be removed.<sup>17</sup>

To solve this, the CMG module of the KUWAY was designed with two CMGs as shown in Figure 7. If the torque generated by the first CMG is denoted as  $T_1$  and the torque generated by the other is denoted as  $T_2$ , the total torque generated by the CMG module is

$$\begin{aligned}\vec{T}_{\text{CMG}} &= \vec{T}_1 + \vec{T}_2 \\ &= \dot{\theta}_{gb1}\omega_1 I_z \cos\theta_{gb1} \vec{i} - \dot{\theta}_{gb1}\omega_1 I_z \sin\theta_{gb1} \vec{k} \\ &\quad + \dot{\theta}_{gb2}\omega_2 I_z \cos\theta_{gb2} \vec{i} - \dot{\theta}_{gb2}\omega_2 I_z \sin\theta_{gb2} \vec{k} \quad (4)\end{aligned}$$

If both flywheels are controlled to rotate with the same magnitude and in opposite direction ( $\omega_1 = -\omega_2 = \omega$ ) and both gimbals are also controlled in the same way

( $\dot{\theta}_{gb1} = -\dot{\theta}_{gb2} = \dot{\theta}_{gb}$ ,  $\theta_{gb1} = -\theta_{gb2} = \theta_{gb}$ ), equation (4) is modified as

$$\vec{T}_{\text{CMG}} = 2\dot{\theta}_{gb}\omega I_z \cos\theta_{gb} \vec{i} \quad (5)$$

If the variation of the gimbal is small around zero, the torque generated by the CMG module is

$$\vec{T}_{\text{CMG}} \approx 2\dot{\theta}_{gb}\omega I_z \vec{i} \quad (6)$$

## Control of the KUWAY

Figure 8 shows the overall control scheme for the KUWAY. It consists of the balancing controller for the two-wheeled self-balancing robot and the CMG controller reducing the effect of disturbances in order to keep a position. The details of each will be explained.

### Balancing controller

In order to get the state space equation, the equations of motion for the self-balancing robot, equations (1) and (2), are linearized around  $\theta = 0$  as

$$\begin{aligned}(Ml_{CG}^2 + I_{CG} + 2n^2 J_m)\ddot{\theta} + (Mrl_{CG} - 2n^2 J_m)\ddot{\phi} \\ + 2n^2 \left(k_f + \frac{k_r k_v}{R}\right)\dot{\theta} - 2n^2 \left(k_f + \frac{k_r k_v}{R}\right)\dot{\phi} - Mgl_{CG}\theta \\ + F_d d = -2n \frac{k_t}{R} V\end{aligned} \quad (7)$$

$$\begin{aligned}[2J + (2m + M)r^2 + 2n^2 J_m]\ddot{\phi} + (Mrl_{CG} - 2n^2 J_m)\ddot{\theta} \\ - 2n^2 \left(k_f + \frac{k_r k_v}{R}\right)\dot{\theta} + 2n^2 \left(k_f + \frac{k_r k_v}{R}\right)\dot{\phi} + F_d r = 2n \frac{k_t}{R} V\end{aligned} \quad (8)$$

That is

$$M' \begin{bmatrix} \ddot{\theta} \\ \ddot{\phi} \end{bmatrix} + C' \begin{bmatrix} \dot{\theta} \\ \dot{\phi} \end{bmatrix} + G' \begin{bmatrix} \theta \\ \phi \end{bmatrix} + W' F_d = TV \quad (9)$$

where  $M'$ ,  $C'$ , and  $G'$  are  $2 \times 2$  matrices and  $W'$  and  $T$  are  $2 \times 1$  vectors. By modifying equation (9), the state space equation is expressed as

$$\begin{aligned}\dot{x} &= Ax + Bu + WF_d \\ y &= Cx\end{aligned} \quad (10)$$

where  $x = [\theta \dot{\theta} \phi \dot{\phi}]^T$ ,  $\dot{x} = [\dot{\theta} \ddot{\theta} \dot{\phi} \ddot{\phi}]^T$ , and  $u = V$ . Since all states are measured,  $C$  is an identical matrix.

If the desired trajectory  $x_r$  is chosen, the desired input  $u_r$  has to satisfy the dynamic equation as

$$\dot{x}_r = Ax_r + Bu_r \quad (11)$$

Then, the error dynamics without the disturbance are expressed by equations (10) and (11) as



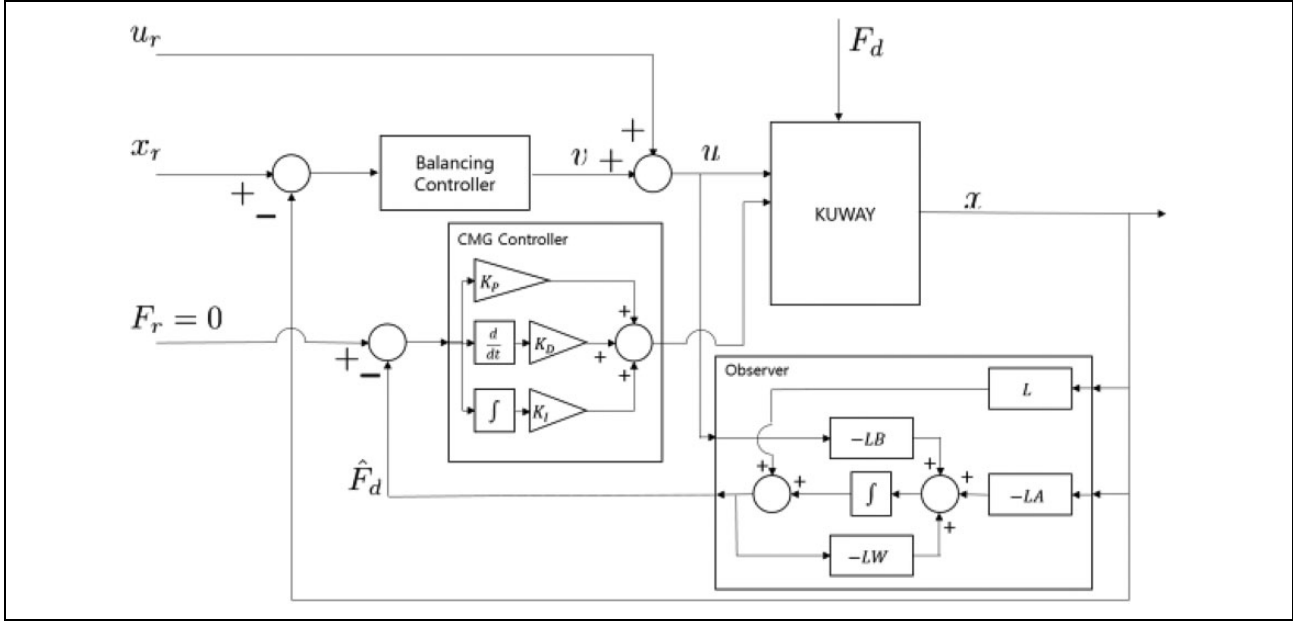


**Figure 8.** Control Scheme for the KUWAY. KUWAY: Kookmin University segWAY.

$$\dot{e} = Ae + Bv \quad (12)$$

where  $e = x_r - x$  and  $v = u_r - u$ . Therefore, the tracking problem can be dealt with at the same time as the regulation problem. In order for the KUWAY to track a desired trajectory, the controller was designed using the linear quadratic regulation method, which minimizes the following performance index<sup>18</sup>

$$\begin{aligned} J &= \int_0^\infty [(x_r(t) - x(t))^T Q (x_r(t) - x(t)) \\ &\quad + u(t)^T R u(t) + 2(x_r(t) - x(t))^T N u(t)] dt \\ &= \int_0^\infty [e(t)^T Q e(t) + u(t)^T R u(t) + 2(e(t))^T N u(t)] dt \end{aligned} \quad (13)$$

where  $Q$  and  $R$  are properly selected as a result of experiment. Therefore, the control law to track the desired trajectory is

$$v = -Ke \quad (14)$$

where  $K$  is a control gain. That is

$$u = u_r + K(x_r - x) \quad (15)$$

### Disturbance observer

Using the controller discussed in the previous section, the normal two-wheeled self-balancing robot was able to maintain its balance even against large disturbances. In order to maintain stability against a disturbance, the robot moved its wheels and tilted its body. However, in terms of safety, it is sometimes necessary for the robot to stay in its position or

minimize movement when a disturbance occurs. To accomplish this, the KUWAY was equipped with the CMG module that reduces the effect of the disturbance. Since there is no sensor to measure the disturbance, the disturbance is estimated by the disturbance observer. Equation (10) can be expressed as

$$\begin{bmatrix} \dot{x} \\ \dot{\hat{F}}_d \end{bmatrix} = \begin{bmatrix} A & W \\ 0 & 0 \end{bmatrix} \begin{bmatrix} x \\ \hat{F}_d \end{bmatrix} + \begin{bmatrix} B \\ 0 \end{bmatrix} u \quad (16)$$

The reduced order observer equations are obtained as

$$\dot{\hat{F}}_d = -LW\hat{F}_d + L(\dot{x} - Ax - Bu) \quad (17)$$

Then

$$\dot{z} = -LW\hat{F}_d - LAx - LBu \quad (18)$$

where  $z = \hat{F}_d - Lx$  and  $L$  is the observer gain.

### CMG controller

When a disturbance occurs, the CMG module of the KUWAY generates a reaction torque that corresponds to the disturbance. The CMG module of the KUWAY operates the gimbal motor using the PID controller, based on feedback regarding the disturbance, as measured by the observer. Since the goal is to eliminate the effects of that disturbance, the desired disturbance  $F_r$  was set to zero. The control gains were determined experimentally. Because the controller uses the observed disturbance, it also includes all sensor noises. Consequently, it was preferable to set the D gain small, because it could amplify the noise of the sensors.

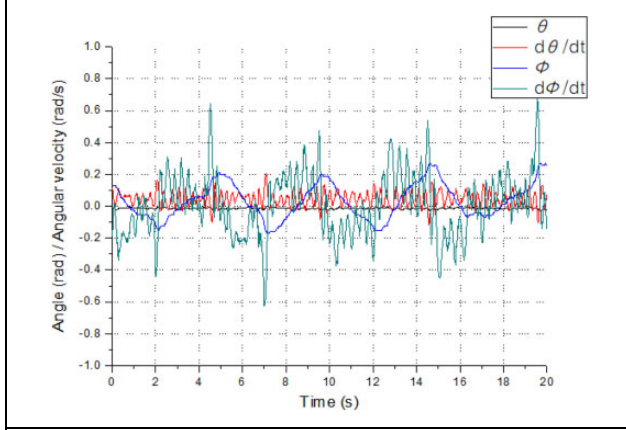


**Figure 9.** The experimental result for the balancing controller.

## Experiment

### Experiment operating the balancing controller

The performance of the balancing controller was verified by the experiment. The control gain was

$$K = \begin{bmatrix} -35.8 & -10.6 & -1.0 & -2.9 \end{bmatrix} \quad (19)$$

when  $Q = \text{diag}(8, 2, 1, 3)$ ,  $R = 1$ , and  $N = 0$ . Since balancing the upper body is more important than maintaining the position of the wheel, the first two parameters of  $Q$  are relatively larger than the others. The detail values are empirically determined. When disturbance wasn't applied to the KUWAY, it kept a balance while the wheels maintained a position without operating the CMG. The experimental results are shown in Figure 9, where the black and red lines represent the angle (Theta:  $\theta$ ) and angular velocity ( $d\theta/dt$ ) of the body, and the blue and green lines represent the angle (Phi:  $\phi$ ) and angular velocity ( $d\phi/dt$ ) of the wheel. In the experiment, the KUWAY maintained balance well with little change in the inclination of the body. On the other hand, the wheels were moved from  $-0.2$  rad to  $0.2$  rad (from  $-11.46^\circ$  to  $11.46^\circ$ ) with approximately  $0.2$  Hz frequency. This movement is thought to have originated with an error in the IMU sensor and a mismatch in the model between the real and ideal robots. Nonetheless, this movement is within an acceptable limit. Therefore, it was verified that the balancing controller maintained the robot's stability.

### Verification of the disturbance observer

Next, the designed disturbance observer was verified by experiment. The actual disturbance was measured using a push-pull gauge to determine the vertical force. Since it is difficult to measure any disturbance when the KUWAY is being controlled, the experiment was conducted without the balancing controller. The wheels were locked and the body was inclined as shown in the left panel of Figure 10.

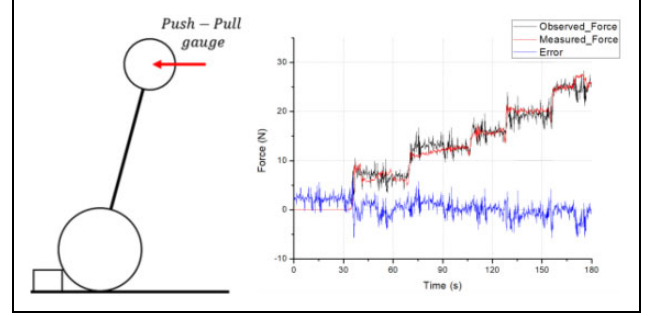


**Figure 10.** Comparison of the estimated observed disturbance and the measured real disturbance.

The body was supported by the push-pull gauge to preserve the inclination. That is, the disturbance was generated and measured using the push-pull gauge. According to the inclination, the disturbance can be changed. The right side of Figure 10 shows the experimental results, where the red line is the real disturbance measured by the push-pull gauge and the black line is the estimated value. Both graphs are very similar to each other. Therefore, the designed disturbance observer was verified to work well.

### Experiment for the CMG module

The performance of the CMG module of the KUWAY was experimentally measured to verify the amount of torque generated. In the experiment, the moment of inertia of the flywheel  $I_{fw}$  was  $5.71 \times 10^{-3} \text{ kgm}^2$ . The two flywheels of the CMG module were set to constantly rotate at 3000 rpm ( $= 314.2 \text{ rad/s}$ ) in opposite directions. The gimbal motor was rotated at 45 rpm ( $= 4.7 \text{ rad/s}$ ). According to equation (6), the ideal torque generated by the CMG module is

$$T_{CMG} \approx 14.8 \text{ Nm} \quad (20)$$

The real torque generated by the CMG module was measured using the push-pull gauge. In the experiment, the wheels were fixed to the body, and the balancing controller was not used to balance the body. The generated torque was converted to the force for the measurement using the push-pull gauge. As shown in Figure 11, the moment arm was set to  $l (= 0.5 \text{ m})$ . The average value of generated torque from several trials was  $15.1 \text{ Nm}$ . The experimental results verified that the CMG module was capable of generating the desired torque.

In addition, another experiment was conducted. In the experiment, the wheels of the KUWAY were locked so that the KUWAY became an inverted pendulum. Then, using only the CMG module, the KUWAY was controlled to maintain balance. The controller was simply designed with a conventional PID controller to regulate the tilt angle of the body. The experimental result is shown in Figure 12. The KUWAY was able to maintain balance with a small variation in tilt angle from  $-0.02$  rad ( $-1.1^\circ$ ) to  $0.03$  rad ( $1.7^\circ$ ).

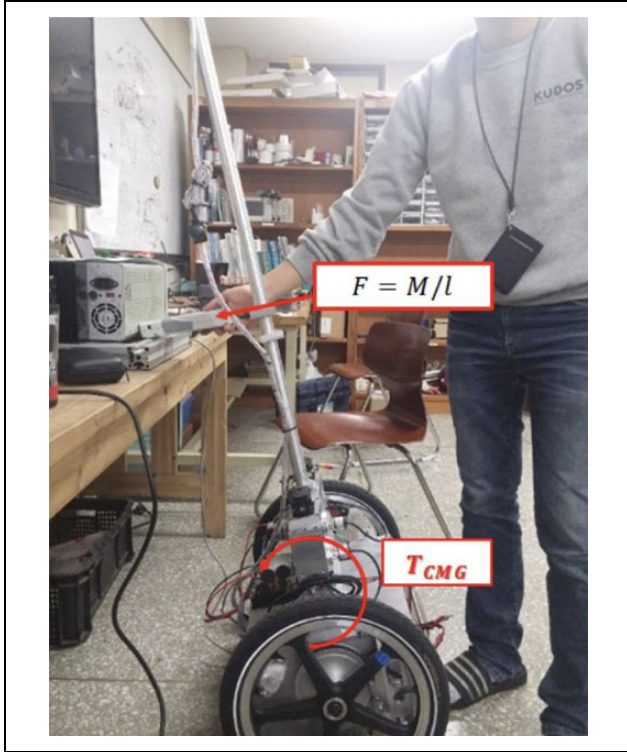


**Figure 11.** Experiment using the CMG module. CMG: control moment gyroscope.

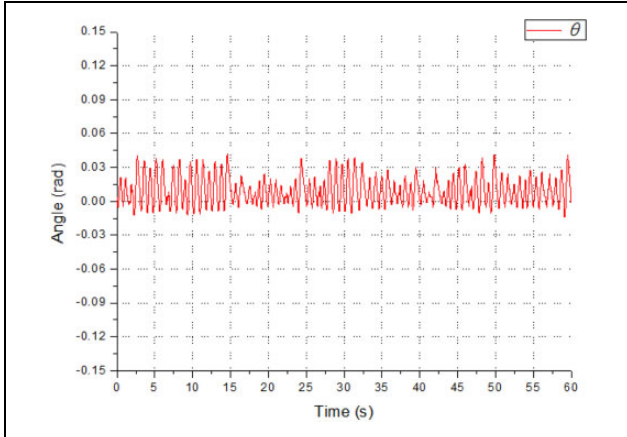


**Figure 12.** Self-balancing experiment using only the CMG module. CMG: control moment gyroscope.

However, it sometimes failed to control the body. In order to generate torque, the gimbal motor has to rotate. Even if the tiny biased disturbance is applied to the robot, the gimbal motor rotates to the specific direction. At last, it will reach to singularity, where the two rotation axes of the flywheels are on a straight line. At this moment, the control fails because no torque is generated by equation (5). For this reason, the CMG module cannot be used continuously but should only be operated for short periods by the time the rotation axes of the flywheels are on the generated torque axes.



**Figure 13.** Disturbance experiment.

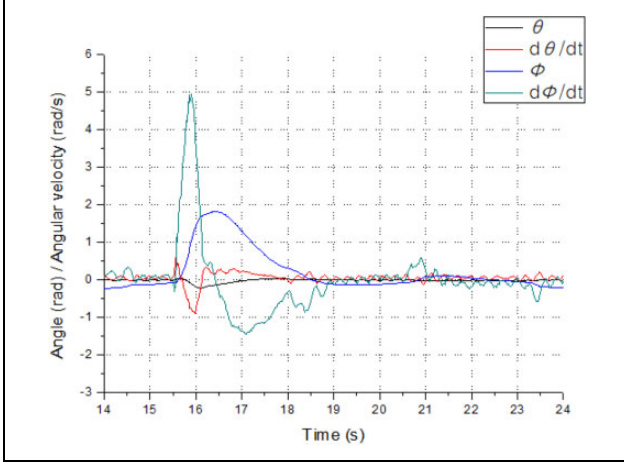
### Experiment for disturbance

In order to observe the effect of the CMG module, two experiments were carried out where the KUWAY maintained balance against a disturbance. In the first experiment, the KUWAY was balanced with just the balancing controller, and in the second experiment, both controllers, the balancing controller and the CMG controller, were applied. Then, the experimental results were compared. The experimental setup is shown in Figure 13. A dead weight of 10 kg was swung from a 25° angle with a moment arm of 0.5 m so that it would hit the robot on the front side.

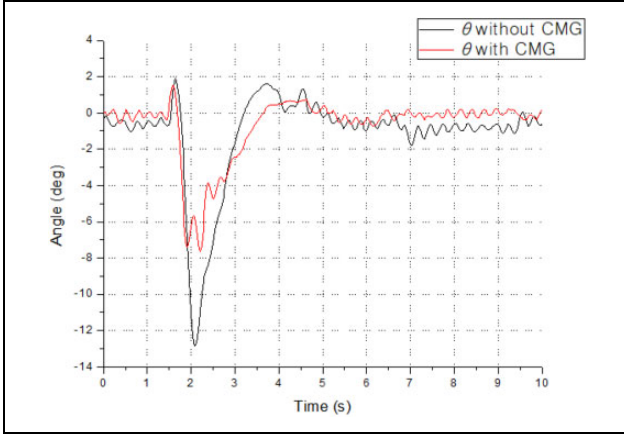
Figure 14 shows the result of the first experiment, confirming that the KUWAY maintained its balance. In this graph,  $\theta$  means angle of the body,  $\dot{\theta}$  means angular velocity of the body,  $\phi$  means angle of the wheels and  $\dot{\phi}$  means angular velocity of the wheels. The black and red lines indicate the angle and angular velocity of the body while the blue and green lines indicate the angle and angular velocity of the wheel. When the dead weight hit the KUWAY at around 1.5 s, the robot's wheels rolled about 1.8 rad (103.13°) in the opposite direction and that means the KUWAY was moved approximately 36 cm backward. Also, the body was tilted up to 12.5° forward as shown by the black line in Figure 15. Then the KUWAY returned to a steady state within 5 s.

Figure 16 shows the results of the second experiment, using both the balancing and CMG controllers, with the same disturbance as before. The CMG controller reduced





**Figure 14.** Results for all aspects in the balancing experiment measuring the response to an inflicted disturbance, using only the balancing controller.



**Figure 15.** Body slope during disturbance experiment without CMG. CMG: control moment gyroscope.

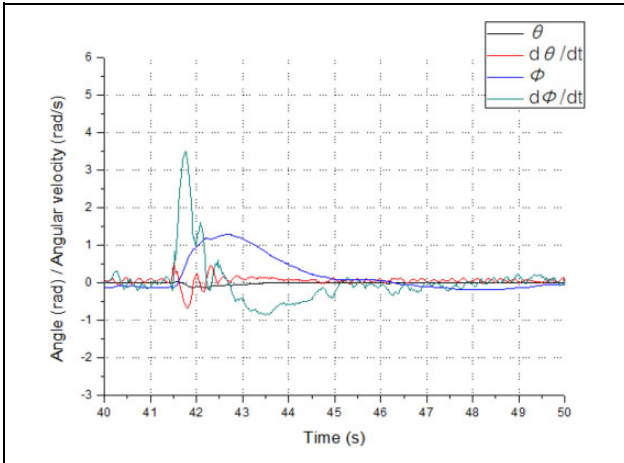


**Figure 16.** Body slope during disturbance experiment with CMG. CMG: control moment gyroscope.

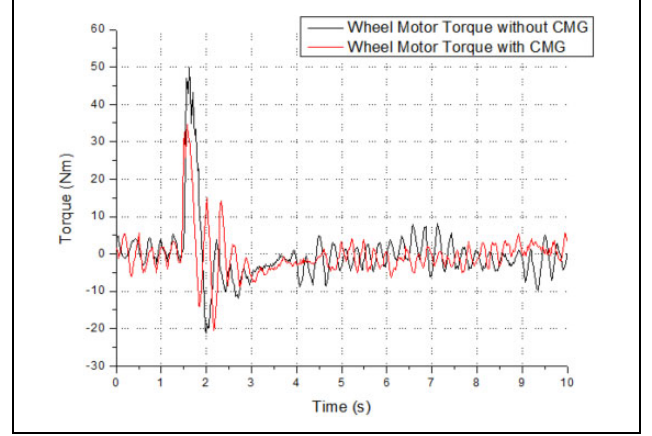


**Figure 17.** Comparison of the wheel motor torque needed to balance the KUWAY. KUWAY: Kookmin University segWAY.

the disturbance while the balancing controller maintained stability. When the dead weight hit the KUWAY at around 1.5 s, the robot moved approximately 28 cm backward while the wheels rolled 1.4 rad (80.21°). Also, the maximum slope of the body was 7.5°, as shown by the red line in Figure 15. Finally, the KUWAY returned to a steady state within 5 s. Therefore, it was clearly demonstrated that the degree of movement of the robot and the angle of the body were reduced when the CMG controller was applied. The improvements were 22.2 and 40.0% in terms of the moving distance and the tilting angle, respectively, calculated with following equation

$$\text{Improvement (\%)} = \frac{\text{value without CMG} - \text{value with CMG}}{\text{value without CMG}} \quad (21)$$

In addition, two experiments were compared in terms of the torque of the motor to drive the wheel. Torque can be calculated based on the motor dynamics, as

$$T_w = n^2 J_m \ddot{\theta} - n^2 J_m \ddot{\phi} + n^2 \left( k_f + \frac{k_t k_v}{R} \right) \dot{\theta} - n^2 \left( k_f + \frac{k_t k_v}{R} \right) \dot{\phi} + \frac{n k_t}{R} V \quad (22)$$

Figure 17 shows the results of the comparison. The black line indicates that up to 50 Nm wheel motor torque was required to maintain balance when only the balancing controller was used. On the other hand, the red line indicates that the maximum torque of the wheel motor was only 35 Nm when the CMG module was used with the balancing controller. The difference is about 15 Nm, and it indicates the maximum torque generated by the CMG module in equation (20). As a result, the maximum necessary torque was reduced by 30.0% by applying the CMG module.

Even though the sum of the generated torques makes no difference, there are effects to reduce a burden of the wheel motors and distribute load of the wheel motor to the CMG

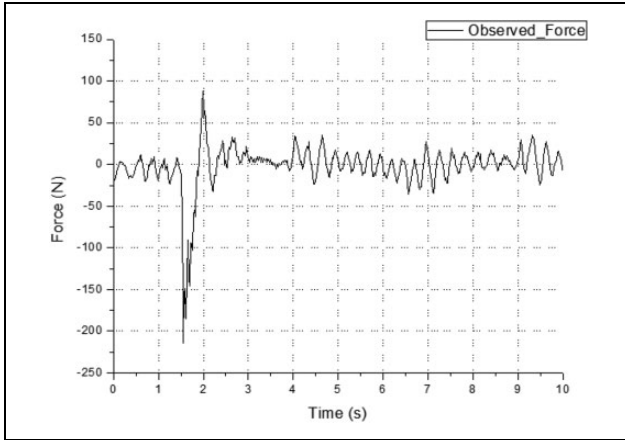


**Figure 18.** The estimated disturbance.

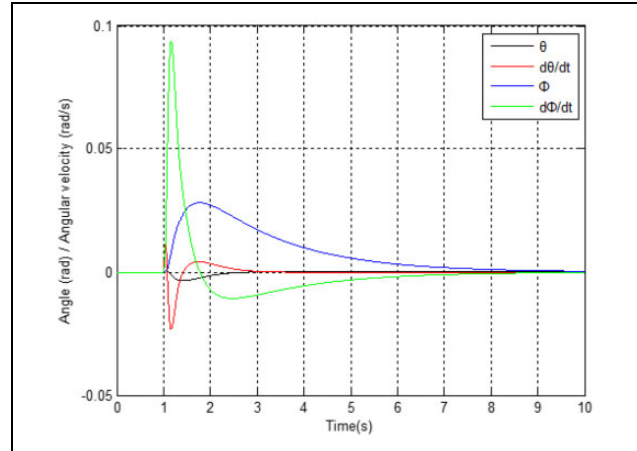
module. If the CMG module generates higher torque, the load on the wheel motor will be correspondingly reduced. For example, the radius of flywheel is increased for higher torque generated by CMG module.

## Discussion

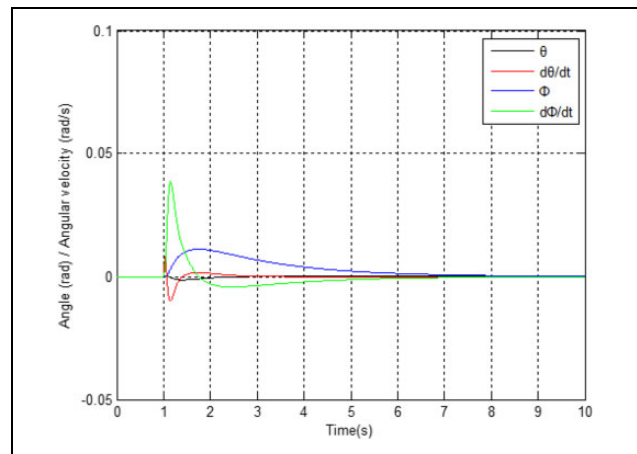
Even though performance was improved by applying the CMG module, the effect of disturbances was not entirely eliminated and the KUWAY was still moved by the disturbances. This is because the CMG module generated an insufficient level of torque based on its hardware specification. Through simulation, it is possible to verify the effect of an improved CMG module.

Figure 18 shows the estimated disturbance for the conditions used in the previous section, where the dead weight hit the KUWAY, based on equation (18). From the figure, the disturbance can be simplified as a constant disturbance with 220 N in magnitude and 50 ms in time duration. Based on the previous model of the KUWAY, a simulation was conducted using the simplified disturbance. In order to verify that the simplified disturbance and the simulation model were correct, the KUWAY was controlled against the disturbance in the simulation with just the balancing controller. Figure 19 shows the result, which is very similar to that in Figure 14. The KUWAY moved about 30 cm (1.5 rad in wheel rotation) backward and the maximum tilt of the body was 11.5°.

In order to verify the effect of the improved CMG module, the diameter of the flywheel was increased 1.5 times in the model, but it was rotated at the same speed. That is, the moment of inertia was increased about 5 times ( $= 1.5^4$ ). A simulation was conducted in which the KUWAY maintained balance using both the balancing and CMG controllers against the disturbance. The simulation results are shown in Figure 20. The maximum distance moved and tilt of the body were reduced to 13 cm (0.64 rad (26.67°) in wheel rotation) and 4.6°, respectively. The performance was improved by 56.7 and 60.0%, respectively. These results confirm that it is possible to guarantee the robots



**Figure 19.** Results of the simulation where the KUWAY was only controlled with the balancing controller against the disturbance. KUWAY: Kookmin University segWAY.



**Figure 20.** The simulation result where the KUWAY controlled with the balancing controller and the improved CMG controller against the disturbance. KUWAY: Kookmin University segWAY; CMG: control moment gyroscope.

stability and safety (small movement) against disturbances when the CMG module generates sufficient torque.

## Conclusion

Usually, a self-balancing robot has to change its position to maintain balance when an external force is applied. This is not a problem if only stability is considered. However, if the robot is in a narrow space, the movement caused by the disturbance can create a real problem. In order to solve this problem, the two-wheeled self-balancing KUWAY robot was developed, incorporating a CMG module. Through experiments, it was confirmed that the CMG module in the KUWAY generated sufficient torque to decrease the effect of the disturbance. In addition, the CMG module distributed the burden of the wheel motors. Even though the CMG module reduced the movement and the tilt of the body of

the experimental robot when a disturbance was applied, the performance was not perfect. Using a simulation, it was verified that the performance was improved using a CMG module which generated higher torque. As following research, the improved CMG module will be developed and applied to experimentally demonstrate the improved performance.

### Declaration of conflicting interests

The author(s) declared no potential conflicts of interest with respect to the research, authorship, and/or publication of this article.

### Funding

The author(s) received no financial support for the research, authorship, and/or publication of this article.

### References

1. Segway, <http://www.segway.com/> (accessed 21 April 2018).
2. Nguyen Hoa G, Morrell J, Mullens KD, et al. Segway robotic mobility platform. In: *Proceedings society of photo-optical instrumentation engineers (SPIE)*, Mobile Robots XVII, 29 December 2004, pp. 207–220.
3. Tsui KM, Desai M, Yanco HA, et al. Exploring use cases for telepresence robots. In: *6th ACM/IEEE international conference on human-robot interaction (HRI)*, Lausanne, 2011, pp. 11–18.
4. Dai F, Gao X, Jiang S, et al. A two-wheeled inverted pendulum robot with friction compensation. *Mechatronics* 2015; 30: 116–125.
5. Stilman TM, Olson J, and Gloss W. Golem krang: dynamically stable humanoid robot for mobile manipulation. In: *IEEE international conference on robotics and automation (ICRA)*, Anchorage, AK, 2010, pp. 3304–3309.
6. Lauwers T, Kantor G, and Hollis R. *One is enough!* San Francisco: International Symposium on Robotics Research, 2005.
7. Choi D, Kim M, and Oh JH. Development of a rapid mobile robot with a multi-degree-of-freedom inverted pendulum using the model-based zero-moment point stabilization method. *Adv Robot* 2012; 26(5–6): 515–535.
8. Lin SC, Tsai CC, and Huang HC. Adaptive robust self-balancing and steering of a two-wheeled human transportation vehicle. *J Intell Robot Syst* 2011; 62(1): 103–123.
9. Ruan X, and Chen J.  $H^\infty$  robust control of self-balancing two-wheeled robot. In: *8th World congress on intelligent control and automation*, Jinan, 2010, pp. 6524–6527.
10. Han HY, Han TY, and Jo HS. Development of omnidirectional self-balancing robot. In: *2014 IEEE international symposium on robotics and manufacturing automation (ROMA)*, Kuala Lumpur, 2014, pp. 57–62. IEEE.
11. Xu J, Shang S, Qi H, et al. Simulative investigation on head injuries of electric self-balancing scooter riders subject to ground impact. *Accid Anal Prev* 2016; 89: 128–141.
12. <http://www.bbc.com/news/uk-england-14167868> (accessed 21 April 2018).
13. Murata boy and murata girl, <http://www.murata.com/about/mboyimgirl/mboy> (accessed 21 April 2018).
14. C-1, <http://litmotors.com/c1/> (accessed 21 April 2018).
15. Kim DKY, Bretney K, Shao A, et al. *US Patent No. 8,532,915*. Washington, DC: US Patent and Trademark Office, 2013.
16. Yetkin H, and Ozguner U. Stabilizing control of an autonomous bicycle. In: *9th Asian control conference (ASCC)*, Istanbul, 2013, pp. 1–6.
17. Chase R. *Analysis of a dual scissored-pair, variable-speed, control moment gyroscope driven spherical robot*. Wayne State University Dissertations. Paper 878, 2014.
18. Cho BK, Kim JH, and Oh JH. Online balance controllers for a hopping and running humanoid robot. *Adv Robot* 2011; 25(9–10): 1209–1225.